Research Article

A Levy solution for bending, buckling, and vibration of Mindlin micro plates with a modified couple stress theory

S. M. Amin Yekani[1] · Famida Fallah[1]

Received: 27 January 2020 / Accepted: 21 November 2020 / Published online: 7 December 2020

Abstract

Based on the modified couple stress and first-order shear deformation plate theories, a Levy-type solution is presented for bending, buckling, and vibration analyses of rectangular isotropic micro plates with simple supports at opposite edges and different boundary conditions at the other two ones. The governing equations are derived using the Hamilton's principle, and then solved by a single Fourier series expansion and the state-space method, which its implementation has not been straightforward. The results are verified with the existing ones for a fully simply supported micro plate in the literature. Finally, the effect of geometric parameters and length scale parameter on bending, buckling, and vibration behaviors of micro plates is studied. Since, there are no analytical solutions for bending, buckling loads, and natural frequencies of Mindlin micro plates with different boundary conditions in the literature and the Navier method is the only available analytical solution for the Mindlin and higher order shear deformable micro plates within the modified couple stress theory, the results presented here can be used as a benchmark in future studies. In addition, it is shown that the difference between results of the Kirchhoff and the Mindlin plate models depends not only on the plate thickness but also on the length scale parameter to thickness ratio (l/h) as well as the boundary supports. This result emphasizes the significance of analytical solutions for shear deformation models of micro plates with different boundary supports.

Keywords Mindlin (first-order shear deformation) plate theory · Modified couple stress theory · Levy method · Bending · Buckling · Free vibration

Mathematics Subject Classification 74N15

1 Introduction

Nowadays, micro-scale structures including beams and plates are widely used in industry and in the micro-electro-mechanical-systems (MEMS) due to their superior mechanical, chemical, and electronic properties [1–3]. Micro plates have a wide variety of applications as actuators or sensors in switches, pressure sensors, micro-pumps, and moving valves [3]. Therefore, there is a crucial need to study the behavior of these structures with sufficient accuracy. In the literature, it is shown that the behavior of micro-scale structures cannot be predicted correctly based on the classical continuum theories and higher order ones are needed. To consider the size effects and overcome the deficiency of the classical continuum models, some non-classical theories have been presented such as micropolar theory [4], non-local elasticity theory [5], strain gradient theory [6], surface elasticity theory [7], classical couple stress theory [8–10] and the modified couple stress theory (MCST) [11]. Based on the non-classical theories, a wide range of recent studies is devoted to investigate the mechanical behavior of size-dependent structures. To

✉ Famida Fallah, fallah@sharif.ir | [1]Department of Mechanical Engineering, Sharif University of Technology, Azadi Ave, P.O. Box 14588-89694, Tehran, Iran.

mention some more recent ones, some researchers used the strain gradient theory to study the behavior of micro/nano beams [12] and plates [13, 14], while some others used the non-local elasticity theory to analyze the size dependent beams [15, 16] and plates [17–19]. Among different non-classical continuum theories, the modified couple stress theory [11] incorporates only one length scale parameter and is preferred over the others due to its simplicity and has been intensively used to study the size dependent structures [20, 21]. Here, the studies on isotropic and homogenous micro plates including bending, buckling, and vibration behaviors using the MCST are reviewed.

Tsiatas [22] studied the bending behavior of a Kirchhoff micro plate with various boundary conditions using a meshless method. Roque et al. [23] carried out the bending analysis of an isotropic Mindlin micro plate using both the Navier method and a meshless method and presented the results for clamped and simply supported plates. Akbaş [24] studied the bending behavior of a Kirchhoff–Love rectangular nano plate using the differential quadrature method. They reported the results for simply supported nano plates. Shaat et al. [25] presented a bending analysis of simply supported Kirchhoff nano plates employing the Navier method. They used surface elasticity theory of Gurtin and Murdoch in conjunction with the MCST in order to include surface effects of nano plates. Based on the Kirchhoff plate theory, Tahani et al. [26] analyzed the free vibration of electrostatically pre-deformed rectangular micro plates using the finite element method. Based on the Kirchhoff plate theory, Yin et al. [27] carried out a vibration analysis of rectangular micro plates employing the Levy method. Jomezadeh et al. [28] performed a vibration analysis of rectangular Kirchhoff micro plates using a Levy-type solution method. Askari and Tahani [29] employed the extended Kantorovich method to analyze the vibration behavior of a Kirchhoff micro plate. They presented the results for a fully clamped micro plate. Asghari and Taati [30] proposed a general model for Kirchhoff micro plates with arbitrary shapes considering the MCST. Ke et al. [31] determined natural frequencies of a Mindlin rectangular micro plate adopting the P-version Ritz method to examine all the possible types of boundary conditions. Ma et al. [32] carried out the bending and free vibration analyses of a simply-supported Mindlin micro plate using the Navier method. Gao et al. [33] presented the Navier solution for bending and vibration analyses of isotropic simply supported micro plates based on the third-order shear deformation theory. Darijani and Shahdadi [34] employed a refined plate theory to analyze the bending and vibration of a rectangular micro plate with simply supported edges, using the Navier method. Lou et al. [35] performed the buckling and post-buckling analyses of piezoelectric hybrid micro plates subjected to thermo-electro-mechanical loads based on the Mindlin plate theory using the Navier method. Based on the MCST and strain gradient theory, Mohammadi and Fooladi Mahani [36] determined the buckling loads of Kirchhoff micro plates using the Levy method. They compared the results obtained within the two mentioned theories and studied the effects of length scale parameters on buckling loads. Mirsalehi et al. [37] used spline finite strip method to study the stability of a Kirchhoff micro plate. Akgöz and Civalek [38] investigated the bending, buckling and vibration of a size dependent Kirchhoff plate embedded in a Winkler's elastic medium using the Navier method. Zhang et al. [39] used finite element method to study the bending, buckling, and free vibration of Mindlin micro plates based on the MCST. It is to be emphasized that boundary supports have significant influence on the mechanical behavior of plates and many attempts have been reported to study this effect via the Galerkin [14], Meshless [22], finite element [26, 39], Levy [27, 28], and spline finite strip [37] methods.

The classical plate theory (CPT) based on the Kirchhoff assumptions provides reliable results for thin plates since the transverse shear effect is neglected in this theory. To overcome shortcomings of the CPT, many shear deformation plate theories are introduced. Mindlin [40] and Reissner [41] proposed displacement-based and stress-based first-order shear deformation theories (FSDT), respectively, which result in constant transverse shear stresses and need shear correction factor. Reissner [42] was the first who uncoupled the six-order equations governing the mechanical behavior of isotropic homogenous plates within FSDT into edge-zone and interior equations. Recently, Nosier and Fallah [43, 44] and Fallah et al. [45] carried out such an uncoupling for tenth-order equations within FSDT, governing linear [43] and nonlinear [44] bending behavior of FG plates as well as stability of sandwich shells [45]. Here, since the deflection, the first three natural frequencies, and buckling load of thin and moderately thick homogenous isotropic plates are reported, the FSDT (Mindlin theory) is accurate enough, however, in order to accurately model FG, composite, and sandwich beams, plates, and shells and overcome the drawbacks of the FSDT, many higher-order shear deformation theories were proposed. More recently, there are attempts to reduce the number of unknowns and remove the need to shear correction factor in shear deformation theories [46]. Matouk et al. [15] and Bousahla et al. [47] used the integral Timoshenko beam theory with three unknowns which needs a shear correction factor to study the dynamic behavior of nano-beams, while Adda Bedia et al. [12] developed a hyperbolic three-unknown beam theory, which could capture shear deformation effects accurately and does not need any shear correction factor. Boutaleb et al. [19], Joshan et al. [48], and Tounsi et al. [49] employed the idea of considering an unknown integral term in the displacement field (as in [15, 47]) in conjunction with cubic, inverse hyperbolic, and trigonometric shear strain shape functions to have four-variable plate theories which consider transverse shear effects accurately. Sinusoidal and inverse hyperbolic shear strain shape functions as the plate models are used in [13, 50], respectively, which capture shear effects without any need to shear correction factor. The idea of considering the transverse deflection as a sum of two unknown functions representing the bending and shear effects as in [12] in conjunction with cubic and sinusoidal shape functions of transverse shear deformation were employed in [14, 51], respectively, resulting in four unknowns in displacement field while taking into account transverse shear effects.

Due to application of micro and nano plates as actuators and sensors, it is crucial to model them with enough accuracy. While the effects of transverse shear and effects of boundary supports on the mechanical responses of plates are significant, it appears from the literature review that there is no analytical solution for micro plates having different boundary conditions and being modeled within shear deformation plate theories in conjugation with MCST. Even though a Levy-type solution [27, 28, 36], or the extended Kantorovich method [29] has been implemented to analyze Kirchhoff micro plates, the governing equations within the first order or higher order micro plate theories are solved using just the Navier method [32–35] or numerical methods [23, 31, 39]. That is, to the best of authors' knowledge, analytical solutions within shear deformation micro plate theories are available for just simply-supported ones. Since, not only the thickness of micro plate but also the boundary supports have significant effects on accuracy and validity of the Kirchhoff model, there is a gap in the literature for analytical solutions to mechanical behavior of Mindlin micro plates with different boundary conditions within MCST. In this paper, an attempt is made to develop analytical solution for bending, buckling and vibration problems of Mindlin micro plates with different boundary conditions within MCST for the first time. To this end, Hamilton's principle is used to derive the equations governing the bending, buckling and free vibration behavior of a micro plate with arbitrary boundary conditions based on the first-order shear deformation and modified couple stress theories. A Levy-type solution in conjunction with the state-space method is adopted to solve the governing equations for micro plates with two simple supports at opposite edges and arbitrary supports at the other ones. It is to be noted that the adoption of the state-space method in this problem was not straightforward, needed some mathematical operations, and is applicable within other shear deformation theories. Maybe this is the reason that the problem of Mindlin micro plate is not solved via the Levy method until now. The effect of different parameters on center deflections, buckling loads and natural frequencies of the micro plate is studied in detail. The analytical results presented here can be used as a benchmark for future studies.

2 Theoretical formulation

Here, an isotropic rectangular micro plate of length a, width b, and uniform thickness h under transverse ($P(x, y)$) and in-plane loadings ($\hat{N}_{xx}$ and $\hat{N}_{yy}$) is considered. The geometry of the plate, the Cartesian coordinate system and the loadings are shown in Fig. 1.

2.1 Equations of motion and boundary conditions

Based on the Hamilton's principle, the equations of motion of a rectangular micro plate are obtained. This principle can be expressed as [52]:

$$\int_0^t (\delta U + \delta V - \delta K)\mathrm{d}t = 0 \tag{1}$$

where U is the strain energy, K is the kinetic energy, and V is the potential of work done by the external forces which are defined as follows [11]:

$$K = \int_{\overline{V}} \frac{1}{2}\rho\left(\dot{u}_i\dot{u}_i\right)\mathrm{d}\overline{V}, U = \int_{\overline{V}} \frac{1}{2}\left(\sigma_{ij}\varepsilon_{ij} + m_{ij}\chi_{ij}\right)\mathrm{d}\overline{V}, \quad i,j = x,y,z \tag{2a}$$

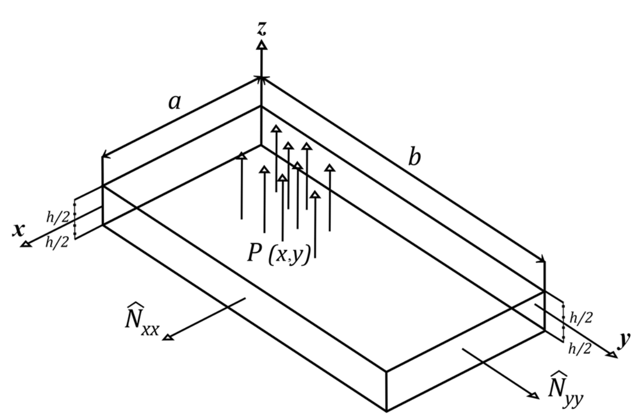

Fig. 1 Geometry of the rectangular plate, the coordinate system, and the loadings

$$V = -\int_A \left(P u_z - \frac{1}{2}\hat{N}_{xx}\left(\frac{\partial u_z}{\partial x}\right)^2 - \frac{1}{2}\hat{N}_{yy}\left(\frac{\partial u_z}{\partial y}\right)^2 \right) \mathrm{d}A \quad (2b)$$

In Eq. (2), u_i are the components of the displacement vector, σ_{ij} and m_{ij} are components of the Cauchy stress tensor and the deviatoric symmetric couple stress tensor, respectively, $\overline{V}$ is the volume of the plate, A denotes the surface of the mid-plane, and a dot over the variable $(\dot{})$ indicates differentiation with respect to time. In addition, in Eq. (2b), the first term in the right hand side of the relation is the potential of work done by the transverse pressure P (considered in bending analysis), while the second and third terms are the work done by the in-plane forces $\hat{N}_{xx}$ and $\hat{N}_{yy}$ in buckling analysis, in which any stretching of the middle plane is ignored and the in-plane forces are assumed to be constant during buckling [53]. Furthermore, the components of strain tensor ε_{ij}, rotation vector θ_i, and symmetric curvature tensor χ_{ij} are defined as follows [52]:

$$\varepsilon_{ij} = \frac{1}{2}\left[u_{i,j} + u_{j,i}\right], \theta_i = \frac{1}{2} e_{ijk} u_{k,j}, \chi_{ij} = \frac{1}{2}\left[\theta_{i,j} + \theta_{j,i}\right], \quad i,j,k = x,y,z \quad (3)$$

where a comma followed by a coordinate variable denotes partial derivative with respect to that variable and e_{ijk} is the permutation symbol.

The displacement field of the first-order shear deformation (Mindlin) plate theory is as follows:

$$\begin{aligned} u_x(x,y,z,t) &= u(x,y,t) - z\psi(x,y,t) \\ u_y(x,y,z,t) &= v(x,y,t) - z\phi(x,y,t) \\ u_z(x,y,z,t) &= w(x,y,t) \end{aligned} \quad (4)$$

where u, v, and w denote the displacements of a point on the mid-plane of the plate along x, y, and z directions, respectively, and ψ and ϕ represent the small rotations of a transverse normal about the y and x axis, respectively.

Upon substitution of Eqs. (4) into (3), the components of strain and curvature fields are obtained as follows:

$$\begin{aligned} &\varepsilon_x = \varepsilon_x^0 + zk_x, \varepsilon_y = \varepsilon_y^0 + zk_y, \varepsilon_z = 0, \\ &\varepsilon_{xy} = \varepsilon_{xy}^0 + zk_{xy}, \varepsilon_{xz} = k_{xz}, \varepsilon_{yz} = k_{yz} \end{aligned} \quad (5a)$$

where

$$\begin{aligned} &\varepsilon_x^0 = \frac{\partial u}{\partial x}, \quad \varepsilon_y^0 = \frac{\partial v}{\partial y}, \quad \varepsilon_{xy}^0 = \frac{1}{2}\left(\frac{\partial u}{\partial y} + \frac{\partial v}{\partial x}\right) \\ &k_x = -\frac{\partial \psi}{\partial x}, \quad k_y = -\frac{\partial \phi}{\partial y}, \quad k_{xy} = -\frac{1}{2}\left(\frac{\partial \psi}{\partial y} + \frac{\partial \phi}{\partial x}\right) \\ &k_{xz} = \frac{1}{2}\left(\frac{\partial w}{\partial x} - \psi\right), \quad k_{yz} = \frac{1}{2}\left(\frac{\partial w}{\partial y} - \phi\right) \end{aligned} \quad (5b)$$

and

$$\chi_x = \chi_x^0, \chi_y = \chi_y^0, \chi_z = \chi_z^0, \chi_{xy} = \chi_{xy}^0, \chi_{xz} = \chi_{xz}^0 + z\chi_{xz}^1, \chi_{yz} = \chi_{yz}^0 + z\chi_{yz}^1 \quad (5c)$$

where

$$\begin{aligned} &\chi_x^0 = \frac{1}{2}\left(\frac{\partial^2 w}{\partial x \partial y} + \frac{\partial \phi}{\partial x}\right), \quad \chi_y^0 = -\frac{1}{2}\left(\frac{\partial^2 w}{\partial x \partial y} + \frac{\partial \psi}{\partial y}\right), \quad \chi_z^0 = -\frac{1}{2}\left(\frac{\partial \phi}{\partial x} - \frac{\partial \psi}{\partial y}\right) \\ &\chi_{xy}^0 = \frac{1}{4}\left(\frac{\partial^2 w}{\partial y^2} + \frac{\partial \phi}{\partial y} - \frac{\partial^2 w}{\partial x^2} - \frac{\partial \psi}{\partial x}\right), \quad \chi_{xz}^0 = \frac{1}{4}\left(\frac{\partial^2 v}{\partial x^2} - \frac{\partial^2 u}{\partial x \partial y}\right), \quad \chi_{yz}^0 = \frac{1}{4}\left(\frac{\partial^2 v}{\partial x \partial y} - \frac{\partial^2 u}{\partial y^2}\right) \\ &\chi_{xz}^1 = -\frac{1}{4}\left(\frac{\partial^2 \phi}{\partial x^2} - \frac{\partial^2 \psi}{\partial x \partial y}\right), \quad \chi_{yz}^1 = -\frac{1}{4}\left(\frac{\partial^2 \phi}{\partial x \partial y} - \frac{\partial^2 \psi}{\partial y^2}\right) \end{aligned} \quad (5d)$$

By substitution of Eq. (5) into Eqs. (1) and (2) and using the fundamental lemma of calculus of variation, the equations of motion of a micro plate subjected to transverse and in-plane loadings are obtained as follows:

$$
\begin{aligned}
&\delta u:\ \frac{\partial N_x}{\partial x}+\frac{\partial N_{xy}}{\partial y}+\frac{1}{2}\frac{\partial^2 H_{xz}}{\partial x\partial y}+\frac{1}{2}\frac{\partial^2 H_{yz}}{\partial y^2}=I_0\frac{\partial^2 u}{\partial t^2}\\
&\delta v:\ \frac{\partial N_y}{\partial y}+\frac{\partial N_{xy}}{\partial x}-\frac{1}{2}\frac{\partial^2 H_{xz}}{\partial x^2}-\frac{1}{2}\frac{\partial^2 H_{yz}}{\partial x\partial y}=I_0\frac{\partial^2 v}{\partial t^2}\\
&\delta \psi:\ \frac{\partial M_x}{\partial x}+\frac{\partial M_{xy}}{\partial y}-Q_x+\frac{1}{2}\frac{\partial H_y}{\partial y}-\frac{1}{2}\frac{\partial H_z}{\partial y}+\frac{1}{2}\frac{\partial H_{xy}}{\partial x}+\frac{1}{2}\frac{\partial^2 G_{xz}}{\partial x\partial y}+\frac{1}{2}\frac{\partial^2 G_{yz}}{\partial y^2}=I_2\frac{\partial^2 \psi}{\partial t^2}\\
&\delta \phi:\ \frac{\partial M_y}{\partial y}+\frac{\partial M_{xy}}{\partial x}-Q_y-\frac{1}{2}\frac{\partial H_x}{\partial x}+\frac{1}{2}\frac{\partial H_z}{\partial x}-\frac{1}{2}\frac{\partial H_{xy}}{\partial y}-\frac{1}{2}\frac{\partial^2 G_{xz}}{\partial x^2}-\frac{1}{2}\frac{\partial^2 G_{yz}}{\partial x\partial y}=I_2\frac{\partial^2 \phi}{\partial t^2}\\
&\delta w:\ \frac{\partial Q_x}{\partial x}+\frac{\partial Q_y}{\partial y}-\frac{1}{2}\frac{\partial^2 H_x}{\partial x\partial y}+\frac{1}{2}\frac{\partial^2 H_y}{\partial x\partial y}-\frac{1}{2}\frac{\partial^2 H_{xy}}{\partial y^2}+\frac{1}{2}\frac{\partial^2 H_{xy}}{\partial x^2}+P=I_0\frac{\partial^2 w}{\partial t^2}-\hat{N}_{xx}\frac{\partial^2 w}{\partial x^2}-\hat{N}_{yy}\frac{\partial^2 w}{\partial y^2}
\end{aligned}
\tag{6}
$$

where the stress and moment resultants and the mass inertias, I_0 and I_2 in Eq. (6) are defined as follows:

$$
\begin{aligned}
&\left(N_x,N_y,N_{xy}\right)=\int_{-\frac{h}{2}}^{\frac{h}{2}}\left(\sigma_{xx},\sigma_{yy},\sigma_{xy}\right)\mathrm{d}z,\ \left(Q_x,Q_y\right)=k^2\int_{-\frac{h}{2}}^{\frac{h}{2}}\left(\sigma_{xz},\sigma_{yz}\right)\mathrm{d}z\\
&\left(M_x,M_y,M_{xy}\right)=\int_{-\frac{h}{2}}^{\frac{h}{2}}\left(\sigma_{xx},\sigma_{yy},\sigma_{xy}\right)z\mathrm{d}z\\
&\left(H_x,H_y,H_{xz},H_{yz},H_{xy},H_z\right)=\int_{-\frac{h}{2}}^{\frac{h}{2}}\left(m_{xx},m_{yy},m_{xz},m_{yz},m_{xy},m_{zz}\right)\mathrm{d}z\\
&\left(G_{xz},G_{yz}\right)=\int_{-\frac{h}{2}}^{\frac{h}{2}}\left(m_{xz},m_{yz}\right)z\mathrm{d}z\\
&I_0=\rho h,\quad I_2=\frac{1}{12}\rho h^3
\end{aligned}
\tag{7}
$$

where k^2 is a shear correction factor. The boundary conditions corresponding to Eq. (6) require the specification of the followings:

$$
\begin{aligned}
&\delta u \text{ or } (N_x+\frac{1}{2}\frac{\partial H_{xz}}{\partial y})n_x+\left(N_{xy}+\frac{1}{2}\frac{\partial H_{xz}}{\partial x}+\frac{1}{2}\frac{\partial H_{yz}}{\partial y}\right)n_y\\
&\delta\frac{\partial u}{\partial y} \text{ or } H_{yz}n_y\\
&\delta v \text{ or } \left(N_{xy}-\frac{1}{2}\frac{\partial H_{xz}}{\partial x}-\frac{1}{2}\frac{\partial H_{yz}}{\partial y}\right)n_x+\left(N_y-\frac{1}{2}\frac{\partial H_{yz}}{\partial x}\right)n_y\\
&\delta\frac{\partial v}{\partial x} \text{ or } H_{xz}n_x\\
&\delta\psi \text{ or } \left(M_x+\frac{1}{2}H_{xy}+\frac{1}{2}\frac{\partial G_{xz}}{\partial y}\right)n_x+\left(M_{xy}+\frac{1}{2}H_y-\frac{1}{2}H_z+\frac{1}{2}\frac{\partial G_{xz}}{\partial x}+\frac{1}{2}\frac{\partial G_{yz}}{\partial y}\right)n_y\\
&\delta\frac{\partial \psi}{\partial y} \text{ or } G_{yz}n_y\\
&\delta\phi \text{ or } \left(M_{xy}-\frac{1}{2}H_x+\frac{1}{2}H_z-\frac{1}{2}\frac{\partial G_{xz}}{\partial x}-\frac{1}{2}\frac{\partial G_{yz}}{\partial y}\right)n_x+\left(M_y-\frac{1}{2}H_{xy}-\frac{1}{2}\frac{\partial G_{yz}}{\partial x}\right)n_y\\
&\delta\frac{\partial \phi}{\partial x} \text{ or } G_{xz}n_x\\
&\delta w \text{ or } \left(Q_x-\frac{1}{2}\frac{\partial H_x}{\partial y}+\frac{1}{2}\frac{\partial H_y}{\partial y}+\frac{1}{2}\frac{\partial H_{xy}}{\partial x}\right)n_x+\left(Q_y-\frac{1}{2}\frac{\partial H_x}{\partial x}+\frac{1}{2}\frac{\partial H_y}{\partial x}-\frac{1}{2}\frac{\partial H_{xy}}{\partial y}\right)n_y\\
&\delta\frac{\partial w}{\partial x} \text{ or } H_{xy}n_x\\
&\delta\frac{\partial w}{\partial y} \text{ or } H_{xy}n_y
\end{aligned}
\tag{8}
$$

where n_x and n_y are the components of an outward unit normal vector to the boundary of the mid-plane.

2.2 Governing equations

The constitutive equations relate the symmetric part of the stress tensor and the deviatoric part of the couple stress tensor to the kinematic parameters as follows [11]:

$$
\sigma_{ij}=\lambda\delta_{ij}\mathrm{tr}(\varepsilon_{ij})+2\mu\varepsilon_{ij},\ m_{ij}=2l^2\mu\chi_{ij}
\tag{9}
$$

where l is a material length scale parameter and λ and μ are the Lamé's constants:

$$\lambda = \frac{E\nu}{(1+\nu)(1-2\nu)}, \mu = \frac{E}{2(1+\nu)} \tag{10}$$

where E and ν are the Young's modulus and the Poisson's ratio, respectively. Upon substitution of Eqs. (5) and (9) into (7) and the subsequent results into the equations of motion (6), the governing equations of motion of a rectangular micro plate are obtained as follows:

$$\begin{aligned}\delta u:\ & A_1\frac{\partial^4 u}{\partial y^4} + A_1\frac{\partial^4 u}{\partial x^2\partial y^2} + A_2\frac{\partial^2 u}{\partial x^2} + A_3\frac{\partial^2 u}{\partial y^2} \\ & - A_1\frac{\partial^4 v}{\partial x^3\partial y} - A_1\frac{\partial^4 v}{\partial x\partial y^3} + A_4\frac{\partial^2 v}{\partial x\partial y} = I_0\frac{\partial^2 u}{\partial t^2}\end{aligned} \tag{11a}$$

$$\begin{aligned}\delta v:\ & -A_1\frac{\partial^4 u}{\partial x^3\partial y} - A_1\frac{\partial^4 u}{\partial x\partial y^3} + A_4\frac{\partial^2 u}{\partial x\partial y} \\ & + A_1\frac{\partial^4 v}{\partial x^4} + A_1\frac{\partial^4 v}{\partial x^2\partial y^2} + A_3\frac{\partial^2 v}{\partial x^2} + A_2\frac{\partial^2 v}{\partial y^2} = I_0\frac{\partial^2 v}{\partial t^2}\end{aligned} \tag{11b}$$

$$\begin{aligned}\delta\psi:\ & A_5\frac{\partial^4\psi}{\partial y^4} + A_5\frac{\partial^4\psi}{\partial x^2\partial y^2} + A_6\frac{\partial^2\psi}{\partial x^2} + A_7\frac{\partial^2\psi}{\partial y^2} + A_3\psi - A_5\frac{\partial^4\phi}{\partial x^3\partial y} \\ & - A_5\frac{\partial^4\phi}{\partial x\partial y^3} + A_8\frac{\partial^2\phi}{\partial x\partial y} + A_1\frac{\partial^3 w}{\partial x^3} + A_1\frac{\partial^3 w}{\partial x\partial y^2} - A_3\frac{\partial w}{\partial x} = I_2\frac{\partial^2\psi}{\partial t^2}\end{aligned} \tag{11c}$$

$$\begin{aligned}\delta\phi:\ & -A_5\frac{\partial^4\psi}{\partial x^3\partial y} - A_5\frac{\partial^4\psi}{\partial x\partial y^3} + A_8\frac{\partial^2\psi}{\partial x\partial y} + A_5\frac{\partial^4\phi}{\partial x^4} \\ & + A_5\frac{\partial^4\phi}{\partial x^2\partial y^2} + A_7\frac{\partial^2\phi}{\partial x^2} + A_6\frac{\partial^2\phi}{\partial y^2} + A_3\phi \\ & + A_1\frac{\partial^3 w}{\partial y^3} + A_1\frac{\partial^3 w}{\partial x^2\partial y} - A_3\frac{\partial w}{\partial y} = I_2\frac{\partial^2\phi}{\partial t^2}\end{aligned} \tag{11d}$$

$$\begin{aligned}\delta w:\ & A_1\frac{\partial^3\psi}{\partial x^3} + A_1\frac{\partial^3\psi}{\partial x\partial y^2} - A_3\frac{\partial\psi}{\partial x} + A_1\frac{\partial^3\phi}{\partial y^3} + A_1\frac{\partial^3\phi}{\partial x^2\partial y} \\ & - A_3\frac{\partial\phi}{\partial y} + A_1\frac{\partial^4 w}{\partial x^4} + A_1\frac{\partial^4 w}{\partial y^4} + 2A_1\frac{\partial^4 w}{\partial x^2\partial y^2} + A_3\frac{\partial^2 w}{\partial x^2} \\ & + A_3\frac{\partial^2 w}{\partial y^2} + P = I_0\frac{\partial^2 w}{\partial t^2} + \hat{N}_{xx}\frac{\partial^2 w}{\partial x^2} + \hat{N}_{yy}\frac{\partial^2 w}{\partial y^2}\end{aligned} \tag{11e}$$

where the coefficients $A_i\,(i = 1, 2, \ldots, 10)$ are presented in "Appendix 1".

3 The solution

The linear partial differential equations in (11) are solved by the Levy method for a micro plate with simple supports at two opposite edges and arbitrary supports at the other ones. Here, it is assumed that edges at $y = 0$ and $y = b$ are simply supported. It is worth mentioning that u and v appear just in Eqs. (11a, b), i.e. extension and bending are decoupled in isotropic plates which results in $u = v = 0$ in bending analysis of a rectangular plate with homogenous boundary conditions. On the other hand, in buckling analysis, the mid-plane stretching is ignored and in vibration analysis, only the bending vibration is taken into account. Therefore, in the remaining, only Eqs. (11c, d, e) are considered.

According to Eqs. (8), the boundary conditions associated with Eqs. (11c, d, e) for simply-supported edges at $y = 0$ and $y = b$, are reduced to what follows:

$$w = H_{xy} = \psi = G_{yz} = M_y - \frac{1}{2}H_{xy} - \frac{1}{2}\frac{\partial G_{yz}}{\partial x} = 0 \tag{12}$$

The boundary conditions along the other two edges at $x = 0$ and $x = a$ (associated with Eqs. (11c, d, e)) can be simply supported (S), clamped (C), or free (F) which their relations according to Eqs. (8) are:

$$\begin{aligned}& S:\ w = H_{xy} = M_x + \frac{1}{2}H_{xy} + \frac{1}{2}\frac{\partial G_{xz}}{\partial y} = \phi = G_{xz} = 0 \\ & C:\ w = \frac{\partial w}{\partial x} = \psi = \phi = \frac{\partial\phi}{\partial x} = 0 \\ & F:\ Q_x - \frac{1}{2}\left(\frac{\partial H_x}{\partial y} - \frac{\partial H_y}{\partial y} - \frac{\partial H_{xy}}{\partial x}\right) = H_{xy} = M_x + \frac{1}{2}H_{xy} + \frac{1}{2}\frac{\partial G_{xz}}{\partial y} = \\ & M_{xy} - \frac{1}{2}\left(H_x - H_z + \frac{\partial G_{xz}}{\partial x} + \frac{\partial G_{yz}}{\partial y}\right) = G_{xz} = 0 \\ & T_{xz} = 0\end{aligned} \tag{13}$$

Using the Levy's methoto satisfy Eqs. (12) and based on a harmonic motion assumption, the displacement field variables ψ, ϕ, and w. are assumed as follows [52]:

$$\begin{aligned}& \psi(x,y,t) = \sum_{m=1}^{\infty}\psi_m(x)\sin\left(\frac{m\pi y}{b}\right)e^{i\omega_m t}, \phi(x,y,t) = \sum_{m=1}^{\infty}\phi_m(x)\cos\left(\frac{m\pi y}{b}\right)e^{i\omega_m t} \\ & w(x,y,t) = \sum_{m=1}^{\infty}w_m(x)\sin\left(\frac{m\pi y}{b}\right)e^{i\omega_m t}\end{aligned} \tag{14}$$

where i is the imaginary unit ($i^2 = -1$), w_m, ψ_m, and ϕ_m are unknown functions of x and ω_m is the natural frequency which is set to zero in bending and buckling analyses. In addition, the transverse load *P(x, y)* in bending analysis is expanded as follows [52]:

$$P(x,y) = \sum_{m=1}^{\infty} P_m(x)\sin\left(\frac{m\pi y}{b}\right) \tag{15}$$

where $P_m(x) = (2/b)\int_0^b P(x,y)\sin\left(\frac{m\pi y}{b}\right)dy$. Substituting Eqs. (14) and (15) into Eqs. (11) yields three ordinary differential equations with total order of ten as follows:

$$\delta\psi\ :\ B_1\psi_m'' + B_2\psi_m + B_3\phi_m''' + B_4\phi_m' + B_5 w_m''' + B_6 w_m' = -I_2\omega_m^2\psi_m \tag{16a}$$

$$\delta\phi\ :\ -B_3\psi_m''' - B_4\psi_m' + B_7\phi_m'''' + B_8\phi_m'' + B_9\phi_m + B_{10}w_m'' + B_{11}w_m = -I_2\omega_m^2\phi_m \tag{16b}$$

$$\delta w\ :\ B_5\psi_m''' + B_{12}\psi_m' - B_{10}\phi_m'' - B_{11}\phi_m + B_5 w_m'''' + B_{13}w_m'' + B_{14}w_m = -P_m - I_0\omega_m^2 w_m + \hat{N}_{xx}w_m'' - \left(\frac{m\pi}{b}\right)^2\hat{N}_{yy}w_m \tag{16c}$$

where the coefficients $B_i, (i = 1\ldots 12)$ are defined in "Appendix 2". There is a problem for solving Eqs. (16) via a state-space method [54]. That is, the highest derivative of ψ_m (which is a third-order derivative) is appearing in Eqs. (16b, c). To overcome this problem, Eq. (16a) is differentiated and the subsequent result is used to eliminate ψ_m''' from Eqs. (16b, c) as follows:

$$\delta\phi\ :\ \left(\frac{B_3B_2}{B_1} - B_4\right)\psi_m' + \left(\frac{B_3^2}{B_1} + B_7\right)\phi_m'''' + \left(\frac{B_3B_4}{B_1} + B_8\right)\phi_m'' + B_9\phi_m + \frac{B_3B_5}{B_1}w_m'''' + \left(\frac{B_3B_6}{B_1} + B_{10}\right)w_m'' + B_{11}w_m = -I_2\frac{B_3}{B_1}\omega_m^2\psi_m' - I_2\omega_m^2\phi_m \tag{17a}$$

$$\delta w\ :\ \left(-\frac{B_5B_2}{B_1} + B_{12}\right)\psi_m' - \frac{B_5B_3}{B_1}\phi_m'''' - \left(\frac{B_5B_4}{B_1} + B_{10}\right)\phi_m'' - B_{11}\phi_m - \left(\frac{B_5^2}{B_1} - B_5\right)w_m'''' - \left(\frac{B_5B_6}{B_1} - B_{13}\right)w_m'' + B_{14}w_m = -P_m + \frac{B_5}{B_1}I_2\omega_m^2\psi_m' + \hat{N}_{xx}w_m'' - \left(I_0\omega_m^2 + \left(\frac{m\pi}{b}\right)^2\hat{N}_{yy}\right)w_m \tag{17b}$$

Table 1 Dimensionless center deflection of a simply supported square micro plate (SSSS) subjected to uniform and sinusoidal loads

Load	$\frac{l}{h} = 0.2$		$\frac{l}{h} = 0.5$		$\frac{l}{h} = 1$	
	Present $\times 10^{-7}$	Roque et al. [23]$\times 10^{-7}$	Present $\times 10^{-7}$	Roque et al. [23]$\times 10^{-7}$	Present $\times 10^{-8}$	Roque et al. [23]$\times 10^{-8}$
Uniform	2.71218	2.7122	1.87752	1.8775	9.00619	9.0062
Sinusoidal	1.71710	1.7171	1.18876	1.1888	5.70624	5.7062

Table 2 Dimensionless buckling load parameter of a simply supported square micro plate (SSSS) ($a = b = 10h, k^2 = 5/6, E = 14.4\times 10^9\text{Pa}, \rho = 12.2\times 10^3\text{Kg/m}^3$)

Buckling mode	$\frac{l}{h} = 0.2$		$\frac{l}{h} = 0.6$		$\frac{l}{h} = 1$	
	Present	Thai et al. [56]	Present	Thai et al. [56]	Present	Thai et al. [56]
Uniaxial buckling	41.52137	41.5214	83.65426	83.6543	163.65389	163.6539
Biaxial buckling	20.76068	20.7607	41.82713	41.8271	81.82694	81.8269

Table 3 First two dimensionless natural frequencies of a simply supported square micro plate (SSSS), ($a = b = 10h, k^2 = 5/6, E = 14.4 \times 10^9 \text{Pa}, \rho = 12.2 \times 10^3 \text{Kg/m}^3$)

Mode	$\frac{l}{h} = 0.2$		$\frac{l}{h} = 0.6$		$\frac{l}{h} = 1$	
	Present	Thai et al. [56]	Present	Thai et al. [56]	Present	Thai et al. [56]
First mode	6.35589	6.3559	9.02611	9.0261	12.63602	12.6360
Second mode	15.10635	15.1064	21.36480	21.3648	29.45879	29.4588

Table 4 Dimensionless center deflection of a square micro plate subjected to uniform and sinusoidal loads

Type of boundary conditions	Load	$l = 0$	$\frac{l}{h} = 0.2$	$\frac{l}{h} = 0.4$	$\frac{l}{h} = 0.6$	$\frac{l}{h} = 0.8$	$\frac{l}{h} = 1$
SSSS	Uniform	2.6676	2.4410	1.9460	1.4561	1.0785	0.8106
	Sinusoidal	1.6889	1.5453	1.2320	0.9220	0.6831	0.5136
SSSC	Uniform	1.8696	1.7093	1.3620	1.0198	0.7566	0.5701
	Sinusoidal	1.2191	1.1147	0.8885	0.6653	0.4937	0.3722
SSCC	Uniform	1.3188	1.2045	0.9593	0.7187	0.5342	0.4038
	Sinusoidal	0.8949	0.8176	0.6515	0.4882	0.3629	0.2743
SSFF	Uniform	9.9621	8.4118	6.2519	4.6492	3.5073	2.7072
	Sinusoidal	4.9521	4.2384	3.2028	2.4023	1.8193	0.4064
SSSF	Uniform	5.9059	5.0614	3.7889	2.7855	2.0654	1.5655
	Sinusoidal	3.1371	2.7269	2.0753	2.0754	1.1446	0.8686
SSCF	Uniform	4.3460	3.7034	2.7480	2.0079	1.4840	1.1235
	Sinusoidal	2.2976	1.9902	1.5058	1.1111	0.8249	0.6257

Now, Eq. (16a), (17a, b) can be reduced to a system of first-order equations with total order of ten as presented in Eq. (18), because the highest order derivatives of ψ_m, ϕ_m, and w_m (which are, respectively, second-order, fourth-order and fourth-order derivatives) appear in the associated equations, i.e. in Eqs. (16a), (17a, b), respectively.

$$\{Z'\} = [A]\{Z\} + \{q\} \tag{18}$$

where

$$\{Z\}^T = \left[\psi_m, \frac{d\psi_m}{dx}, \phi_m, \frac{d\phi_m}{dx}, \frac{d^2\phi_m}{d^2x}, \frac{d^3\phi_m}{d^3x}, w_m, \frac{dw_m}{dx}, \frac{d^2w_m}{dx^2}, \frac{d^3w_m}{dx^3}\right] \tag{19}$$

and the matrix $[A]$ and the load vector $\{q\}$ are presented in "Appendix 3". It is worth mentioning that the buckling loads, $\hat{N}_{xx}$, $\hat{N}_{yy}$ and the natural frequency, ω_m appear in matrix $[A]$ as some unknowns in buckling and vibration analyses. The general solution of Eq. (18) is as follows [54]:

$$\{Z\} = [U][D]\{C\} + [U][D]\int^{x} [D]^{-1}[U]^{-1}\{q\} \tag{20}$$

where $[U]$ is the matrix of eigenvectors of $[A]_{10\times10}$, $\{C\}_{10\times1}$ is the vector of integration constants and $[D]_{10\times10}$ is the diagonal matrix defined as follows:

Table 5 Dimensionless center deflection of a square micro plate subjected to uniform and sinusoidal loadings ($l/h = 1$)

Type of boundary conditions	Load	$\frac{a}{h} = 5$	$\frac{a}{h} = 10$	$\frac{a}{h} = 15$
SSSS	Uniform	1.1927	0.8903	0.8314
	Sinusoidal	0.7705	0.5678	0.5278
SSSC	Uniform	0.9473	0.6570	0.5937
	Sinusoidal	0.6289	0.4311	0.3882
SSCC	Uniform	0.7570	0.4893	0.4276
	Sinusoidal	0.5196	0.3330	0.2905
SSFF	Uniform	3.3963	2.8493	2.7362
	Sinusoidal	1.7967	1.4881	1.4240
SSSF	Uniform	2.0979	1.6799	1.5904
	Sinusoidal	1.1922	0.9385	0.8846
SSCF	Uniform	1.6619	1.2510	1.1547
	Sinusoidal	0.9548	0.7032	0.6452

$$[D] = \text{diag}\left(e^{\lambda_1 x}, e^{\lambda_2 x}, \dots, e^{\lambda_{10} x}\right) \tag{21}$$

where $\lambda_i (i = 1 \dots 10)$ are eigenvalues of $[A]$.

3.1 Bending analysis

In bending analysis, the in-plane forces $\hat{N}_{xx}$, $\hat{N}_{yy}$ and all the time derivatives and consequently ω_m are set to zero.

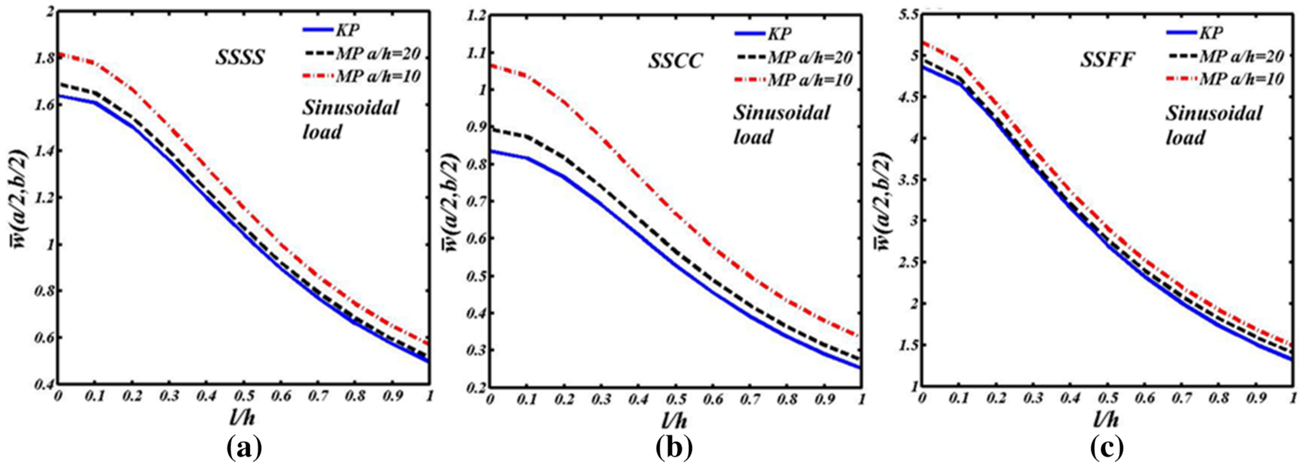

Fig. 2 Variations of dimensionless center deflection of **a** SSSS, **b** SSCC, **c** SSFF square micro plate under sinusoidal loading versus l/h ratio and its comparison with the results of Kirchhoff micro plate

Table 6 Dimensionless center deflection of a rectangular micro plate subjected to uniform and sinusoidal loads ($l/h = 1, b = 20h$)

Type of boundary conditions	Load	$\frac{a}{b} = \frac{1}{2}$	$\frac{a}{b} = 1$	$\frac{a}{b} = 2$	$\frac{a}{b} = 3$
SSSS	Uniform	2.1190	0.8106	0.1247	0.0297
	Sinusoidal	1.3846	0.5136	0.0811	0.0202
SSSC	Uniform	1.1282	0.5701	0.1146	0.0290
	Sinusoidal	0.7790	0.3722	0.0759	0.0199
SSCC	Uniform	0.6659	0.4038	0.1049	0.0284
	Sinusoidal	0.4927	0.2743	0.0708	0.0197
SSFF	Uniform	42.5410	2.7072	0.1647	0.0319
	Sinusoidal	21.4617	1.4064	0.0963	0.0208
SSSF	Uniform	5.0194	1.5655	0.1444	0.0308
	Sinusoidal	2.7078	0.8686	0.0886	0.0205
SSCF	Uniform	4.1618	1.1235	0.1338	0.0302
	Sinusoidal	2.2176	0.6257	0.0832	0.0203

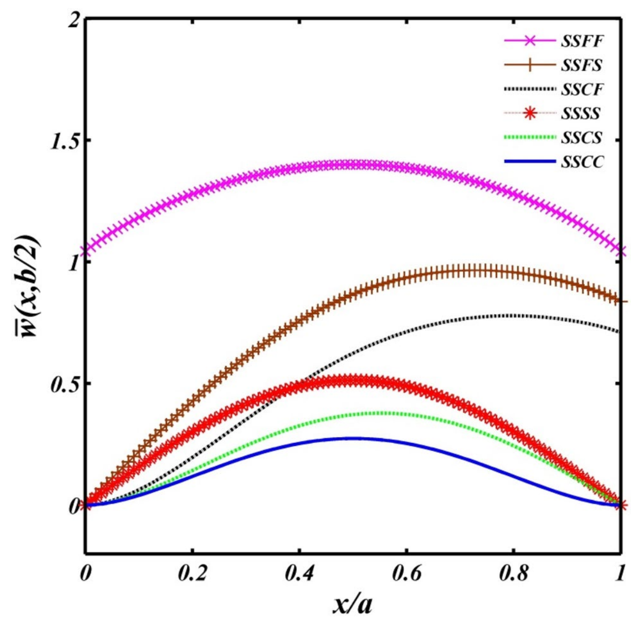

Fig. 3 Dimensionless deflection of a square micro plate under sinusoidal load along x axis for various boundary conditions ($l/h = 1$)

Therefore, there isn't any unknown in matrix $[A]$ (see Eqs. (26) and (29) in "Appendix 3"). To find the integration constants, any arbitrary combination of boundary conditions at edges $x = 0, a$ presented in Eq. (13) is imposed which yields inhomogeneous algebraic equations in terms of integration constants.

3.2 Buckling analysis

In buckling analysis, the transverse load P_m and all the time derivatives and consequently ω_m are set to zero, while the buckling load is still unknown in matrix $[A]$ (see Eqs. (26) and (29) in "Appendix 3"). Imposing the appropriate boundary conditions at edges $x = 0, a$ leads to a linear homogeneous system of algebraic equations in terms of integration constants in which the buckling load is still an unknown in the matrix of coefficients. If the determinant of coefficient matrix is set to zero for a nontrivial solution, the bucking load is determined.

3.3 Free vibration

In vibration analysis, all external forces including P, $\hat{N}_{xx}$ and $\hat{N}_{yy}$ are set to zero, while the natural frequency is still an unknown in matrix $[A]$ (see Eqs. (26) and (29) in "Appendix 3"). By setting the determinant of the coefficient matrix

Table 7 Dimensionless buckling load parameter of a square micro plate

Type of boundary conditions		$l=0$	$\frac{l}{h}=0.2$	$\frac{l}{h}=0.4$	$\frac{l}{h}=0.6$	$\frac{l}{h}=0.8$	$\frac{l}{h}=1$
SSSS	Uniaxial	5.9992	6.5563	8.2236	10.9892	14.8334	19.7290
	Biaxial	2.9996	3.2781	4.1118	5.4946	7.4167	9.8645
SSSC	Uniaxial	7.1770	7.8438	9.8368	13.1352	17.7052	23.5005
	Biaxial	3.9382	4.3047	5.3993	7.2105	9.7199	12.9024
SSCC	Uniaxial	9.7714	10.6810	13.3926	17.8640	24.0274	31.7916
	Biaxial	5.5411	6.0587	7.5988	10.1380	13.6383	18.0491
SSFF	Uniaxial	1.7051	2.3773	4.2629	7.2579	11.3030	16.3584
	Biaxial	0.9718	1.2778	1.9692	2.8172	3.8189	5.0169
SSSF	Uniaxial	2.0481	2.8174	4.8933	8.0139	12.0360	16.9097
	Biaxial	1.0119	1.3622	2.2235	3.3631	4.7373	6.3873
SSCF	Uniaxial	2.0483	2.8204	4.9505	8.2707	12.6935	18.1580
	Biaxial	1.0629	1.4380	2.4033	3.7613	5.4393	7.4509

Table 8 Dimensionless buckling load parameter of a square micro plate ($l/h=1$)

Type of boundary conditions		$\frac{a}{h}=5$	$\frac{a}{h}=10$	$\frac{a}{h}=15$
SSSS	Uniaxial	13.1495	17.8455	19.1983
	Biaxial	6.5747	8.9227	9.5991
SSSC	Uniaxial	13.8048	20.4206	22.6006
	Biaxial	7.7592	11.2415	12.4120
SSCC	Uniaxial	16.3376	26.1029	30.0335
	Biaxial	9.4900	14.8921	17.0647
SSFF	Uniaxial	9.6235	14.3270	15.8987
	Biaxial	4.0034	4.7481	4.9412
SSSF	Uniaxial	10.0707	14.6781	16.2265
	Biaxial	4.8969	5.9932	6.2780
SSCF	Uniaxial	10.3866	15.5447	17.3498
	Biaxial	5.5050	6.8978	7.2927

of the linear homogenous system of algebraic equations (obtained by imposing the appropriate boundary conditions) to zero, the natural frequency is determined.

4 Numerical results

For the purpose of numerical illustration, unless mentioned otherwise, the material properties of the plate and its geometry are assumed to be $E = 1.44 \times 10^9 Pa$, $\nu = 0.38$, $\rho = 1.22 \times 10^3 \frac{Kg}{m^3}$, *and* $l = 17.6 \times 10^{-6}$m (which is determined experimentally) [55] and $a = b = 20h$. Also, the shear correction factor is considered to be $k^2 = 0.8$ [23, 32].

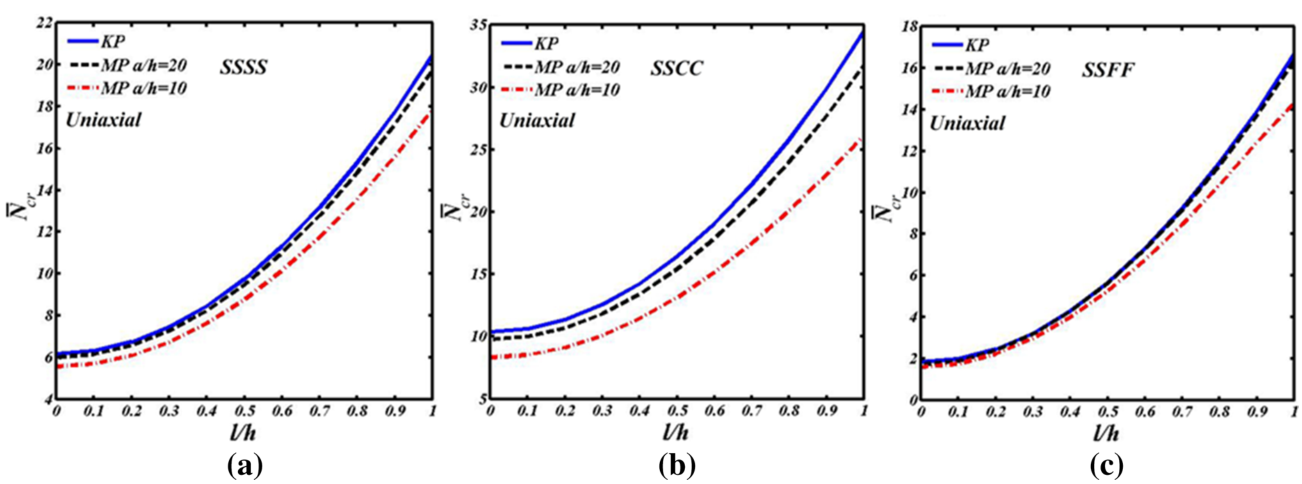

Fig. 4 Variations of dimensionless buckling load of **a** SSSS, **b** SSCC, **c** SSFF square micro plate under uniaxial loading versus l/h ratio and its comparison with the results of Kirchhoff micro plate

4.1 Verification studies

Here, to verify the results of the present study, three examples including bending, buckling, and free vibration of a simply-supported micro plate are provided.

4.1.1 Bending

The dimensionless central deflections ($w(a/2, b/2)/h$) of a fully simply-supported micro plate subjected to sinusoidal ($P(x, y) = 0.1 \sin\left(\frac{n\pi x}{a}\right) \sin\left(\frac{m\pi y}{b}\right)$N/m) and uniform ($P = 0.1$N/m) loadings for different ratios of length scale parameter to thickness are presented in Table 1 and compared with those reported by Roque et al. [23]. Excellent agreement is seen to exist between the results. It is recalled that in reference [23] the bending analysis of an isotropic Mindlin micro plate is carried out using the Navier method.

4.1.2 Buckling

In Table 2, the dimensionless buckling loads ($N_{cr}(a^2/Eh^3)$) of a fully simply supported Mindlin micro plate under uniaxial $\left(\hat{N}_{xx} = N_{cr}, \hat{N}_{yy} = 0\right)$ and biaxial $\left(\hat{N}_{xx} = \hat{N}_{yy} = N_{cr}\right)$ in-plane compressive forces are presented and compared with those reported in Ref. [56]. It is again seen that the Levy solution presented here for the buckling analysis is in excellent agreement with the Navier solution in [56].

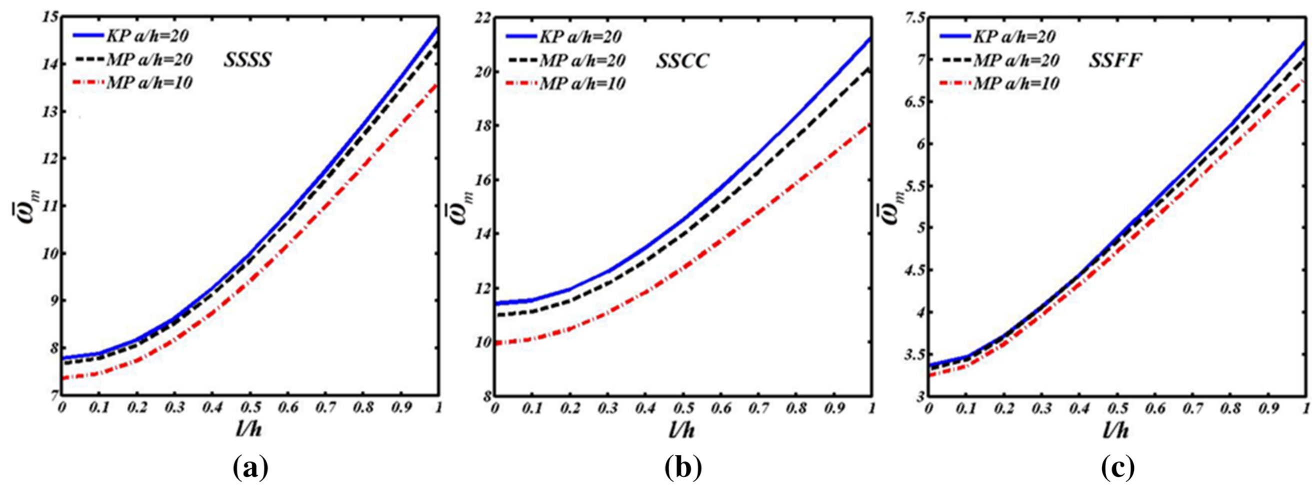

Fig. 5 Variations of dimensionless fundamental frequencies of **a** SSSS, **b** SSCC, **c** SSFF square micro plate versus l/h ratio and its comparison with the results of Kirchhoff micro plate

Table 9 Dimensionless two first frequencies ($m = 1$) of a square micro plate

Type of boundary conditions		$l = 0$	$\frac{l}{h} = 0.2$	$\frac{l}{h} = 0.4$	$\frac{l}{h} = 0.6$	$\frac{l}{h} = 0.8$	$\frac{l}{h} = 1$
SSSS	First mode	7.6798	8.0699	9.1375	10.6735	12.4950	14.4814
	Second mode	18.7894	19.7053	22.2114	25.8086	30.0516	34.6388
SSSC	First mode	9.1078	9.5629	10.8039	12.5853	14.6947	16.9879
	Second mode	21.9079	22.9773	25.8671	29.9952	34.8388	40.0407
SSCC	First mode	10.9932	11.5349	13.0003	15.1011	17.5798	20.2623
	Second mode	25.3303	26.5798	29.9016	34.6166	40.1124	45.9685
SSFF	First mode	3.3240	3.7071	4.4416	5.2534	6.1161	7.0254
	Second mode	5.0090	5.8522	7.6049	9.6167	11.7281	13.8955
SSSF	First mode	3.9327	4.4449	5.4487	6.5800	7.7896	9.0607
	Second mode	10.0431	10.8307	12.8265	15.4841	18.4750	21.6331
SSCF	First mode	4.1947	4.7673	5.9050	7.1863	8.5446	9.9615
	Second mode	11.9279	12.8023	15.0382	18.0493	21.4522	25.0406

Table 10 Dimensionless first- and second-mode frequencies of a square micro plate, ($l/h = 1, m = 1$)

Type of boundary conditions		$\frac{a}{h} = 5$	$\frac{a}{h} = 10$	$\frac{a}{h} = 15$
SSSS	First mode	11.4784	13.6242	14.2387
	Second mode	23.6268	30.6944	33.4206
SSSC	First mode	12.7629	15.6274	16.5814
	Second mode	25.8991	34.4253	38.2087
SSCC	First mode	14.3136	18.1244	19.5911
	Second mode	28.3041	38.3359	43.3586
SSFF	First mode	6.1817	6.7839	6.9677
	Second mode	11.2180	13.1112	13.6672
SSSF	First mode	7.7320	8.6919	8.9650
	Second mode	16.1861	19.8767	21.1067
SSCF	First mode	8.2608	9.4518	9.8228
	Second mode	17.7902	22.4515	24.2277

4.1.3 Free vibration

In Table 3, the first two dimensionless natural frequencies $\left(\omega_m\left(\frac{a^2}{h}\sqrt{\frac{\rho}{E}}\right)\right)$ of a fully simply supported Mindlin micro plate in the plane-stress state are given and compared to those presented in Ref. [56] in which the Navier method is employed. It is seen that the results are in excellent agreement [56].

4.2 Parametric studies

Here, the bending, buckling and free vibration of micro plates with different boundary conditions subjected to two types of loadings; sinusoidal $P = P_0 \sin\left(\frac{n\pi x}{a}\right)\sin\left(\frac{m\pi y}{b}\right)$ and uniform $P = P_0$ loadings are considered. Recall that the two edges at $y = 0$ and $y = b$ are simply supported and the others can have simple support (S), clamped support (C), or free edge (F). For convenience, the following dimensionless parameters are introduced:

$$\overline{w} = \frac{100Eh^3}{P_0a^4}w(a/2, b/2), \overline{\omega}_m = \omega_m\frac{a^2}{h}\sqrt{\frac{\rho}{E}}, \overline{N}_{cr} = \left(N_{cr}\frac{a^2}{Eh^3}\right) \tag{22}$$

4.2.1 Bending

The dimensionless center deflection, $\overline{w}$ of micro plates with six possible types of boundary conditions subjected to both sinusoidal and uniform loadings are obtained and presented in Tables 4 and 5. In Table 4, various ratios of material length scale parameter to thickness ($l/h = 0, 0.2, 0.4, 0.6, 0.8, 1$) are considered and in Table 5 the effect of side-to-thickness ratio ($a/h = 5, 10, 15$) is studied. The variations of dimensionless center deflection of micro plates with three types of boundary conditions (SSSS, SSCC and SSFF) and two ratios of $a/h = 10, 20$ versus l/h ratio are depicted in Fig. 2 and compared with the results of Kirchhoff micro plate ($K^2 \to \infty$). In Table 4 and Fig. 2, it is observed that the classical continuum theory ($l = 0$) overestimates the deflection and by increasing the length scale parameter (l/h), the deflections of micro plates with all types of boundary supports become smaller, i.e. the micro plate becomes stiffer. In Table 5 and Fig. 2, it is seen that as the ratio of (a/h) increases, i.e. the micro plate becomes thinner; the dimensionless deflection decreases because it is nondimensionalized as in (22), however, the deflection per se increases, as expected. In addition, it is seen in Fig. 2 that the difference between the Kirchhoff micro plate (KP) and the Mindlin micro plate (MP) exists even for a thin plate (MP) especially for SSCC micro plate and this difference for all types of boundary supports increases as the micro plate becomes thicker or as l/h ratio reduces.

In Table 6, the effect of aspect ratio (a/b) on dimensionless center deflection, $\overline{w}$ of micro plates with various types of boundary conditions subjected to both sinusoidal and uniform loadings are studied. It is observed that by increasing the aspect ratio (a/b), the dimensionless deflection (see Eq. (22)) reduces while the deflection per se increases, as expected.

Variations of dimensionless deflection of a square micro plate under sinusoidal load along x axis for all six possible boundary conditions are shown in Fig. 3. In Fig. 3 and Tables 4, 5, and 6, it is expectedly seen that as the boundaries become more rigid, the deflections decrease, e.g. among three types of boundary conditions SSFF, SSCF and SSSF, plates with SSFF supports have the largest deflections and plates with SSFC supports have the smallest ones.

4.2.2 Buckling

Dimensionless buckling load, $\overline{N}_{cr}$, of a micro plate with six possible types of boundary conditions subjected to uniaxial $\left(\hat{N}_{xx} = N_{cr}, \hat{N}_{yy} = 0\right)$ and biaxial in-plane compressive forces ($\hat{N}_{xx} = \hat{N}_{yy} = N_{cr}$) for different ratios of length scale parameter to thickness ($l/h = 0, 0.2, 0.4, 0.6, 0.8, 1$) and side-to-thickness ratio ($a/h = 5, 10, 15$) are obtained and presented in Tables 7 and 8, respectively. The variations of buckling load of a plate under uniaxial loading versus l/h ratio for three types of boundary conditions (SSSS, SSCC and SSFF) and two ratios of $a/h = 10 and 20$ are presented in Fig. 4 and compared with those of Kirchhoff micro plate ($K^2 \to \infty$). In Table 7 and Fig. 4, it is observed that the classical continuum theory ($l = 0$) underestimates the buckling load and increasing the length scale parameter (l/h)

or using more rigid boundaries leads to a stiffer micro plate and larger buckling loads. In Table 8 and Fig. 4, it is seen that as the ratio of (a/h) increases, i.e. the micro plate becomes thinner; the dimensionless buckling load increases because it is nondimensionalized as in (22), while the buckling load per se decreases. In addition, it is seen in Fig. 4 that the difference between the Kirchhoff micro plate (KP) and the Mindlin micro plate (MP) is more pronounced in SSCC micro plates and this difference for all types of boundary supports increases as the micro plate becomes thicker or as l/h ratio increases. The differences in buckling loads predicted by the Kirchhoff and the Mindlin plate models for $a/h = 20$ (which is considered to be a thin plate and results of the Kirchhoff model is valid for) and $l/h = 1$ are 8.5%, 3.7%, and 2.1% for, respectively, SSCC, SSSS, and SSFF boundary conditions.

4.2.3 Vibration

Two first dimensionless frequencies, $\overline{\omega}_m$, of square micro plates with six possible types of boundary conditions for different ratios of length scale parameter to thickness $(l/h = 0, 0.2, 0.4, 0.6, 0.8, 1)$ and side-to-thickness ratio $(a/h = 5, 10, 15)$ are presented in Tables 9 and 10, respectively. In addition, the variations of fundamental dimensionless frequency in terms of l/h for three types of boundary conditions (SSSS, SSCC and SSFF) and two ratios of $a/h = 10, 20$ are presented in Fig. 5 and compared with those of Kirchhoff micro plate $(K^2 \to \infty)$. In Table 9 and Fig. 5, it is observed that the classical continuum theory $(l = 0)$ underestimates the natural frequencies and increasing the length scale parameter (1/*h*) or using more rigid boundaries leads to a stiffer micro plate and larger natural frequencies. In Table 10 and Fig. 5, it is seen that as the ratio of (a/h) increases, the dimensionless frequencies (see Eq. (22)) increases, while the natural frequencies per se decrease. In addition, it is seen in Fig. 4 that the difference between natural frequencies within the Kirchhoff micro plate (KP) and the Mindlin micro plate (MP) is more pronounced in SSCC plates. This difference for all types of boundary supports increases as the micro plate becomes thicker (as expected) or as l/h ratio increases. For $a/h = 20$ and $l/h = 1$, the differences between fundamental frequencies within the Kirchhoff and the Mindlin plate models are 5.1%, 2.1%, and 2.8% for, respectively, SSCC, SSSS, and SSFF boundary supports.

5 Conclusion

In this study, bending, buckling, and free vibration behavior of a rectangular micro plate is studied considering the modified couple stress theory and first-order shear deformation plate theory. The equations of motion are derived using the Hamilton's principle and solved by the Levy's method and the state-space method. However, some mathematical operations are necessary to render the state-space method feasible. The results are verified with the ones available for fully simply supported micro plates in the literature. The Levy's solution available in the literature for micro-plates is limited to the Kirchhoff micro-plates. Consequently, the results presented here for the Mindlin micro-plates with different boundary conditions using an analytical approach can serve as a benchmark and are more accurate than the results within the Kirchhoff theory for thicker plates (even for a micro-plate with $a/h = 20$). The difference in results obtained by the Kirchhoff and the Mindin plate models depends not only on the plate thickness but also on the length scale parameter to thickness ratio (l/h) as well as on the boundary supports. This difference is more pronounced in SSCC boundary supports and for higher ratios of l/h, the difference in results of natural frequencies and buckling loads between the Kirchhoff and the Mindlin plate theories increases. In addition, the numerical results show that the fundamental frequencies and buckling loads increase (and transverse deflection decreases) with increasing the l/h ratio and decreasing the side-to-thickness ratio (a/h). Furthermore, more rigid boundary conditions increase frequencies and buckling loads and reduce the transverse deflection, as expected. It is to be noted that the micro plates considered in this study are limited to the ones with the two opposite edges simply supported and arbitrary conditions of support on the remaining edges. Presenting semi-analytical solutions for micro plates with completely arbitrary boundary conditions should be addressed in future studies.

Availability of data and materials All authors contributed to the study conception and design. Material preparation, data collection and analysis were performed by Famida Fallah and Seyed Mohammad Amin Yekani. The first draft of the manuscript was written by Seyed MohammadAmin Yekani and all authors commented on previous versions of the manuscript. All authors read and approved the final manuscript.

Code availability MATLAB software.

Compliance with ethical standards

Conflict of interest The authors declare that they have no conflict of interest.

Appendix 1

The coefficients appearing in Eqs. (11) are defined as follows:

$$A_1=-\frac{1}{4}hl^2\mu, A_2=h(\lambda+2\mu), A_3=k^2h\mu, A_4=h\lambda+k^2h\mu, A_5=\frac{1}{48}h^3l^2\mu,$$
$$A_6=-\frac{h^3}{12}(\lambda+2\mu)-\frac{1}{4}hl^2\mu, A_7=-\frac{h^3}{12}\mu-hl^2\mu, A_8=-\frac{h^3}{12}(\lambda+\mu)+\frac{3}{4}hl^2\mu, \tag{23}$$

Appendix 2

The coefficients appearing in Eqs. (16) are defined as follows:

$$\begin{aligned}
&B_1=-\frac{h^3}{12}(\lambda+2\mu)-\left(\frac{m\pi}{b}\right)^2\frac{l^2\mu h^3}{48}-\frac{l^2\mu h}{4},\\
&B_2=\left(\frac{m\pi}{b}\right)^2\left(\frac{h^3}{12}\mu+l^2\mu h\right)+k^2\mu h+\left(\frac{m\pi}{b}\right)^4\frac{l^2\mu h^3}{48}, B_3=\left(\frac{m\pi}{b}\right)\frac{l^2\mu h^3}{48},\\
&B_4=\left(\frac{m\pi}{b}\right)\left(\lambda\frac{h^3}{12}+\mu\frac{h^3}{12}-\left(\frac{m\pi}{b}\right)^2\frac{l^2\mu h^3}{48}-\frac{3l^2\mu h}{4}\right), B_5=-\frac{l^2\mu h}{4},\\
&B_6=-k^2\mu h+\left(\frac{m\pi}{b}\right)^2\frac{l^2\mu h}{4}, B_7=\frac{l^2\mu h^3}{48}, B_8=-\frac{h^3}{12}\mu-\left(\frac{m\pi}{b}\right)^2\frac{l^2\mu h^3}{48}-hl^2\mu,\\
&B_9=\left(\frac{m\pi}{b}\right)^2\left(\frac{h^3}{12}(\lambda+2\mu)+\frac{l^2\mu h}{4}\right)+k^2\mu h, B_{10}=-\left(\frac{m\pi}{b}\right)\frac{l^2\mu h}{4},\\
&B_{11}=-\left(\frac{m\pi}{b}\right)\left(k^2\mu h-\left(\frac{m\pi}{b}\right)^2\frac{l^2\mu h}{4}\right), B_{12}=-k^2\mu h+\left(\frac{m\pi}{b}\right)^2\frac{l^2\mu h}{4},\\
&B_{13}=k^2\mu h+\left(\frac{m\pi}{b}\right)^2\frac{l^2\mu h}{2}, B_{14}=-\left(\frac{m\pi}{b}\right)^2\left(k^2\mu h+\left(\frac{m\pi}{b}\right)^2\frac{l^2\mu h}{4}\right)
\end{aligned} \tag{24}$$

where

$$E_1=-\frac{B_2}{B_1}-\frac{I_2\omega_m^2}{B_1}, E_2=-\frac{B_4}{B_1}, E_3=-\frac{B_3}{B_1}, E_4=-\frac{B_6}{B_1}, E_5=-\frac{B_5}{B_1} \tag{26}$$

and the coefficients $E_{ij}(i=1,2\text{and}j=1\ldots6)$ are the components of matrix $[E]_{2\times6}$ which is obtained as follows:

$$[E]=[F]^{-1}[G] \tag{27}$$

where

$$[F]=\begin{bmatrix}-\left(\frac{B_3^2}{B_1}+B_7\right) & -\frac{B_3B_5}{B_1}\\ \frac{B_5B_3}{B_1} & \frac{B_5^2}{B_1}-B_5\end{bmatrix}, \tag{28}$$

$$[G]=\begin{bmatrix}\frac{B_3B_2}{B_1}-B_4+\frac{B_3}{B_1}I_2\omega_m{}^2 & B_9+I_2\omega_m{}^2 & \frac{B_3B_4}{B_1}+B_8 & B_{11} & \frac{B_3B_6}{B_1}+B_{10} & 0\\ B_{12}-\frac{B_5B_2}{B_1}+\frac{B_5}{B_1}I_2\omega_m{}^2 & -B_{11} & -\left(\frac{B_5B_4}{B_1}+B_{10}\right) & B_{14}+I_0\omega_m{}^2+\left(\frac{m\pi}{b}\right)^2\widehat{N}_{yy} & B_{13}-\frac{B_5B_6}{B_1}-\widehat{N}_{xx} & P_m\end{bmatrix}. \tag{29}$$

Appendix 3

The matrix $[A]$ and the load vector $\{q\}$ appearing in Eq. (18) are defined as follows:

$$[A]=\begin{bmatrix}0&1&0&0&0&0&0&0&0&0\\ E_1&0&0&E_2&0&E_3&0&E_4&0&E_5\\ 0&0&0&1&0&0&0&0&0&0\\ 0&0&0&0&1&0&0&0&0&0\\ 0&0&0&0&0&1&0&0&0&0\\ 0&E_{11}&E_{12}&0&E_{13}&0&E_{14}&0&E_{15}&0\\ 0&0&0&0&0&0&0&1&0&0\\ 0&0&0&0&0&0&0&0&1&0\\ 0&0&0&0&0&0&0&0&0&1\\ 0&E_{21}&E_{22}&0&E_{23}&0&E_{24}&0&E_{25}&0\end{bmatrix}, \{q\}=\begin{bmatrix}0\\0\\0\\0\\0\\E_{16}\\0\\0\\0\\E_{26}\end{bmatrix} \tag{25}$$

References

1. Hassanpour PA, Cleghorn WL, Esmailzadeh E, Mills JK (2007) Vibration analysis of micro-machined beam-type

resonators. J Sound Vib 308:287–301. https://doi.org/10.1016/j.jsv.2007.07.043
2. Batra RC, Porfiri M, Spinello D (2008a) Vibrations of narrow microbeams predeformed by an electric field. J Sound Vib 309:600–612. https://doi.org/10.1016/j.jsv.2007.07.030
3. Batra RC, Porfiri M, Spinello D (2008b) Vibrations and pull-in instabilities of micro electromechanical von kármán elliptic plates incorporating the Casimir force. J Sound Vib 315:939–960. https://doi.org/10.1016/j.jsv.2008.02.008
4. Eringen AC (1967) Theory of micropolar plates. Z Angew Math Phys 18:12–30. https://doi.org/10.1007/BF01593891
5. Eringen AC (1972) Non local polar elastic continua. Int J Eng Sci 10:1–16. https://doi.org/10.1016/0020-7225(72)90070-5
6. Aifantis EC (1999) Strain gradient interpretation of size effects. Int J Fract 95:1–4. https://doi.org/10.1023/A:1018625006804
7. Gurtin ME, Weissmuller J, Larche F (1998) The general theory of curved deformable interfaces in solids at equilibrium. Philos Mag A 78:1093–1109. https://doi.org/10.1080/014186198253138
8. Cosserat E, Cosserat F (1909) Theorie des corps deformables. Hermann et Fils, Paris. https://doi.org/10.1038/081067a0
9. Toupin RA (1962) Elastic materials with couple-stresses. Arch Ration Mech Anal 11:385–414. https://doi.org/10.1007/BF00253945
10. Mindlin RD, Tiersten HF (1962) Effects of couple-stresses in linear elasticity. Arch Ration Mech Anal 11:415–448. https://doi.org/10.1007/BF00253946
11. Yang F, Chong ACM, Lam DCC, Tong P (2002) Couple stress based strain gradient theory for elasticity. Int J Solids Struct 39:2731–2743. https://doi.org/10.1016/S0020-7683(02)00152-X
12. Adda BW, Houari MSA, Bessaim A, Bousahla AA, Tounsi A, Saeed T, Alhodaly MS (2019) A new hyperbolic two-unknown beam model for bending and buckling analysis of a nonlocal strain gradient nanobeams. J Nano Res 57:175–191. https://doi.org/10.4028/www.scientific.net/JNanoR.57.175
13. Akgöz B, Civalek O (2015) A microstructure-dependent sinusoidal plate model based on the strain gradient elasticity theory. Acta Mech 226:2277–2294. https://doi.org/10.1007/s00707-015-1308-4
14. Karami B, Janghorban M, Tounsi A (2019) Galerkin's approach for buckling analysis of functionally graded anisotropic nanoplates/different boundary conditions. Eng Commun 35:1297–1316. https://doi.org/10.1007/s00366-018-0664-9
15. Matouk H, Bousahla AA, Heireche H, Bourada F, Adda Bedia EA, Tounsi A, Mahmoud SR, Tounsi A, Benrahou KH (2020) Investigation on hygro-thermal vibration of P-FG and symmetric S-FG nanobeam using integral Timoshenko beam theory. Adv Nano Res 8:293–305. https://doi.org/10.12989/anr.2020.8.4.293
16. Berghouti H, Adda Bedia EA, Benkhedda A, Tounsi A (2019) Vibration analysis of nonlocal porous nanobeams made of functionally graded material. Adv Nano Res 7:351–364. https://doi.org/10.12989/anr.2019.7.5.351
17. Bellal M, Hebali H, Heireche H, Bousahla AA, Tounsi A, Bourada F, Mahmoud SR, Adda Bedia EA, Tounsi A (2020) Buckling behavior of a single-layered graphene sheet resting on viscoelastic medium via nonlocal four-unknown integral model. Steel Compos Struct 34:643–655. https://doi.org/10.12989/scs.2020.34.5.643
18. Balubaid M, Tounsi A, Dakhel B, Mahmoud SR (2019) Free vibration investigation of FG nanoscale plate using nonlocal two variables integral refined plate theory. Comput Conc 24:579–586. https://doi.org/10.12989/cac.2019.24.6.579
19. Boutaleb S, Benrahou KH, Bakora A, Algarni A, Bousahla AA, Tounsi A, Tounsi A, Mahmoud SR (2019) Dynamic analysis of nanosize FG rectangular plates based on simple nonlocal quasi 3D HSDT. Adv Nano Res 7:191–208. https://doi.org/10.12989/anr.2019.7.3.191
20. Khorshidi MA (2019) Effect of nano-porosity on postbuckling of non-uniform microbeams. SN Appl Sci 1:677. https://doi.org/10.1007/s42452-019-0704-0
21. Akgöz B, Civalek Ö (2017) Effects of thermal and shear deformation on vibration response of functionally graded thick composite microbeams. Compos Part B Eng 129:77–87. https://doi.org/10.1016/j.compositesb.2017.07.024
22. Tsiatas GC (2009) A new Kirchhoff plate model based on a modified couple stress theory. Int J Solids Struct 46:2757–2764. https://doi.org/10.1016/j.ijsolstr.2009.03.004
23. Roque CMC, Ferreira AJM, Reddy JN (2013) Analysis of Mindlin microplates with a modified couple stress theory and a meshless method. Appl Math Model 37:4626–4633. https://doi.org/10.1016/j.apm.2012.09.063
24. Akbaş SD (2016) Static analysis of a nano plate by using generalized differential quadrature method. Int J Eng Appl Sci 8:30–39. https://doi.org/10.24107/ijeas.252143
25. Shaat M, Mahmoud FF, Gao XL, Faheem AF (2014) Size-dependent bending analysis of Kirchhoff nano-plates based on a modified couple-stress theory including surface effects. Int J Mech Sci 79:31–37. https://doi.org/10.1016/j.ijmecsci.2013.11.022
26. Tahani M, Askari AR, Mohandes Y, Hassani B (2015) Size-dependent free vibration analysis of electrostatically pre-deformed rectangular micro-plates based on the modified couple stress theory. Int J Mech Sci 94–95:185–198. https://doi.org/10.1016/j.ijmecsci.2015.03.004
27. Yin L, Qian Q, Wang L, Xia W (2010) Vibration analysis of microscale plates based on modified couple stress theory. Acta Mech Solida Sinica 23:386–393. https://doi.org/10.1016/S0894-9166(10)60040-7
28. Jomehzadeh E, Noori HR, Saidi AR (2011) The size-dependent vibration analysis of micro-plates based on a modified couple stress theory. Physica E 43:877–883. https://doi.org/10.1016/j.physe.2010.11.005
29. Askari AR, Tahani M (2015) Analytical determination of size-dependent natural frequencies of fully clamped rectangular microplates based on the modified couple stress theory. J Mech Sci Tech 29:2135–2145. https://doi.org/10.1007/s12206-015-0435-0
30. Asghari M, Taati E (2012) A size-dependent model for functionally graded micro-plates for mechanical analyses. J Vib Cont 19:1614–1632. https://doi.org/10.1177/2F1077546312442563
31. Ke L-L, Wang Y-S, Yang J, Kitipornchai S (2012) Free vibration of size-dependent Mindlin microplates based on the modified couple stress theory. J Sound Vib 331:94–106. https://doi.org/10.1016/j.jsv.2011.08.020
32. Ma HM, Gao X-L, Reddy JN (2011) A non-classical Mindlin plate model based on a modified couple stress theory. Acta Mech 220:217–235. https://doi.org/10.1007/s00707-011-0480-4
33. Gao X-L, Huang JX, Reddy JN (2013) A non-classical third-order shear deformation plate model based on a modified couple stress theory. Acta Mech 224:2699–2718. https://doi.org/10.1007/s00707-013-0880-8
34. Darijani H, Shahdadi AH (2015) A new shear deformation model with modified couple stress theory for microplates. Acta Mech 226:2773–2788. https://doi.org/10.1007/s00707-015-1338-y
35. Lou J, He L, Du J, Wu H (2016) Buckling and post-buckling analyses of piezoelectric hybrid microplates subject to thermo-electro-mechanical loads based on the modified couple stress theory. Compos Struct 153:332–344. https://doi.org/10.1016/j.compstruct.2016.05.107
36. Mohammadi M, Fooladi Mahani M (2015) An analytical solution for buckling analysis of size-dependent rectangular micro-plates according to the modified strain gradient and

couple stress theories. Acta Mech 226:3477–3493. https://doi.org/10.1007/s00707-015-1384-5
37. Mirsalehi M, Azhari M, Amoushahi H (2015) Stability of thin FGM microplate subjected to mechanical and thermal loading based on the modified couple stress theory and spline finite strip method. Aero Sci Tech 47:356–366. https://doi.org/10.1016/j.ast.2015.10.001
38. Akgöz B, Civalek Ö (2013) Modeling and analysis of micro-sized plates resting on elastic medium using the modified couple stress theory. Meccanica 48:863–873. https://doi.org/10.1007/s11012-012-9639-x
39. Zhang B, He Y, Liu D, Gan Z, Shen L (2013) A non-classical Mindlin plate finite element based on a modified couple stress theory. Eur J Mech A/Solids 42:63–80. https://doi.org/10.1016/j.euromechsol.2013.04.005
40. Mindlin RD (1951) Influence of rotatory inertia and shear on flexural motions of isotropic elastic plates. ASME J Appl Mech 18:31–38. https://doi.org/10.1007/978-1-4613-8865-4_29
41. Reissner E (1945) The effect of transverse shear deformation on the bending of elastic plates. ASME J Appl Mech 12:68–77. https://doi.org/10.1177/002199836900300316
42. Reissner E (1947) On bending of elastic plate. Q Appl Math 5:55–68. https://doi.org/10.1002/sapm1944231184
43. Nosier A, Fallah F (2008) Reformulation of Mindlin-Reissner governing equations of functionally graded circular plates. Acta Mech 198:209–233. https://doi.org/10.1007/s00707-007-0528-7
44. Nosier A, Fallah F (2009) Non-linear analysis of functionally graded circular plates under asymmetric transverse loading. Int J Non-Linear Mech 44:928–942. https://doi.org/10.1016/j.ijnonlinmec.2009.07.001
45. Fallah F, Taati E, Asghari M (2018) Decoupled stability equation for buckling analysis of FG and multilayered cylindrical shells based on the first-order shear deformation theory. Compos Part B Eng 154:225–241. https://doi.org/10.1016/j.compositesb.2018.07.051
46. Boussoula A, Boucham B, Bourada M, Bourada F, Tounsi A, Bousahla AA, Tounsi A (2020) A simple nth-order shear deformation theory for thermomechanical bending analysis of different configurations of FG sandwich plates. Smart Struct Syst 25:197–218. https://doi.org/10.12989/sss.2020.25.2.197
47. Bousahla AA, Bourada F, Mahmoud SR, Tounsi A, Algarni A, Adda Bedia EA, Tounsi A (2020) Buckling and dynamic behavior of the simply supported CNT-RC beams using an integral-first shear deformation theory. Comput Conc 25:155–166. https://doi.org/10.12989/cac.2020.25.2.155
48. Joshan YS, Grover N, Singh BN (2017) A new non-polynomial four variable shear deformation theory in axiomatic formulation for hygro-thermo-mechanical analysis of laminated composite plates. Compos Struct 182:685–693. https://doi.org/10.1016/j.compstruct.2017.09.029
49. Tounsi A, Al-Dulaijan SU, Al-Osta MA, Chikh A, Al-Zahrani MM, Sharif A, Tounsi A (2020) A four variable trigonometric integral plate theory for hygro-thermo-mechanical bending analysis of AFG ceramic-metal plates resting on a two-parameter elastic foundation. Steel Compos Struct 34:511–524. https://doi.org/10.12989/scs.2020.34.4.511
50. Grover N, Maiti DK, Singh BN (2013) A new inverse hyperbolic shear deformation theory for static and buckling analysis of laminated composite and sandwich plates. Comput Struct 95:667–675. https://doi.org/10.1016/j.compstruct.2012.08.012
51. Tounsi A, Houari MSA, Benyoucef S, Adda Bedia EA (2013) A refined trigonometric shear deformation theory for thermoelastic bending of functionally graded sandwich plates. Aero Sci Technol 24:209–220. https://doi.org/10.1016/j.ast.2011.11.009
52. Reddy JN (2007) Theory and analysis of elastic plates and shells, 2nd edn. Taylor & Francis, New York
53. Timoshenko SP, Gere JM (1963) Theory of elastic stability, 2nd edn. McGraw-Hill, New York
54. Simmons GF, Robertson JS (2017) Differential equations with applications and historical notes, 2nd edn. Taylor & Francis, New York
55. Lam DCC, Yang F, Chong ACM, Wang J, Tong P (2003) Experiments and theory in strain gradient elasticity. J Mech Phys Solids 51:1477–1508. https://doi.org/10.1016/S0022-5096(03)00053-X
56. Thai H-T, Choi D-H (2013) Size-dependent functionally graded Kirchhoff and Mindlin plate models based on a modified couple stress theory. Compos Struct 95:142–153. https://doi.org/10.1016/j.compstruct.2012.08.023